Active damping strategies for control of the E-ELT field stabilization mirror

B. Sedghi[a] and M. Dimmler[a] and M. Müller[a]

[a]European Southern Observatory (ESO), Karl-Schwarzschild-Strasse. 2, Garching, Germany

ABSTRACT

The fifth mirror unit (M5) of the E-ELT is a field stabilization unit responsible to correct for the dynamical tip and tilt caused mainly due to the wind load on the telescope. The unit is composed of: i) an electromechanical subunit, and ii) an elliptical mirror with a size of approximately 2.4 by 3-m. The M5 unit has been designed and prototyped using a three point support for the mirror actuated by piezo actuators without the need of a counter weight system. To be able to meet the requirements of the telescope, i.e. sufficient wavefront rejection capability, the unit shall exhibit a sufficient bandwidth for tip/tilt reference commands. In the presence of the low damped mechanical resonant modes, such a bandwidth can be guaranteed thanks to an active damping loop. In this paper, different active damping strategies for the M5 unit are presented. The efficiency of the approaches are analyzed using a detailed model of the unit. On a scale-one prototype active damping was implemented and the efficiency was demonstrated.

Keywords: E-ELT, field stabilization unit, active damping, control, robust stability

1. INTRODUCTION

The European Extremely Large Telescope (E–ELT) is a project led by ESO for a next generation optical and near–infrared, ground–based telescope. Its optical design is based on a three–mirror anastigmat with two folding flat mirrors sending the beam to either of the two Nasmyth foci along the elevation axis of the telescope[1] ,[2]. The elliptical primary mirror consists of almost 800 off-axis aspherical segments, each 1.45-m in size and 50-mm thick. The secondary and tertiary mirrors are designed as convex and concave aspherical mirrors, respectively, providing active position and shape control. The quarternary mirror is adaptive aiming at the compensation of fast wavefront distortions which are mainly due to atmospheric turbulence. The main purpose of the ultra–lightweight fifth mirror is to provide the compensation of image motion. The opto-mechanical mirror units (M1– M5)[3] are held by the main structure, which also supports the instruments at the Nasmyth platforms, all handling tools and all equipment necessary for the altitude azimuth kinematics. The main structure also holds the pre–focal stations, which contain the on–sky metrology for wavefront control.

The M5 unit of the E-ELT together with the adaptive M4 are responsible for correcting the tip/tilt errors of the telescope mainly due to the atmospheric and wind load perturbations. The entire unit is inclined at 53.5-degrees and mounted on a rotating stage provided by the telescope main structure. The unit is composed of: i) an electromechanical subunit, and ii) a mirror with a size of approximately 2.4 by 3-m. The electromechanical unit is composed of a support unit based on a fixed frame - main structure - that carries the base frame upon which the actuators and the central restraint are located. The M5 electromechanical unit has been designed and prototyped by NTE/CSEM[4] on the basis of a three point actuated support of the mirror without a counter weight system. The actuator is based on a CEDRAT APA[5] design custom built for the E-ELT. A preloaded elliptical steel ring is forced open by the action of a piezo stack running along the major axis. In the relaxed state the actuator is at its maximum extent and expanding the piezo compresses the actuator.

The intrinsic stiffness of the actuator is high (45-N/μm). A position sensor is used to provide absolute calibration and feedback to the actuator. It is mounted on the same flange as the actuator. The position sensor selected is an eddy current device that provides a 15-nm resolution over a 1-mm range. The actuator provides interfaces for accelerometers to be mounted at different locations, e.g. ends of piezo stack, or on top near the

Further author information: (Send correspondence to B. Sedghi)
B. Sedghi: E-mail: bsedghi@eso.org, Telephone: +49 89 32006529

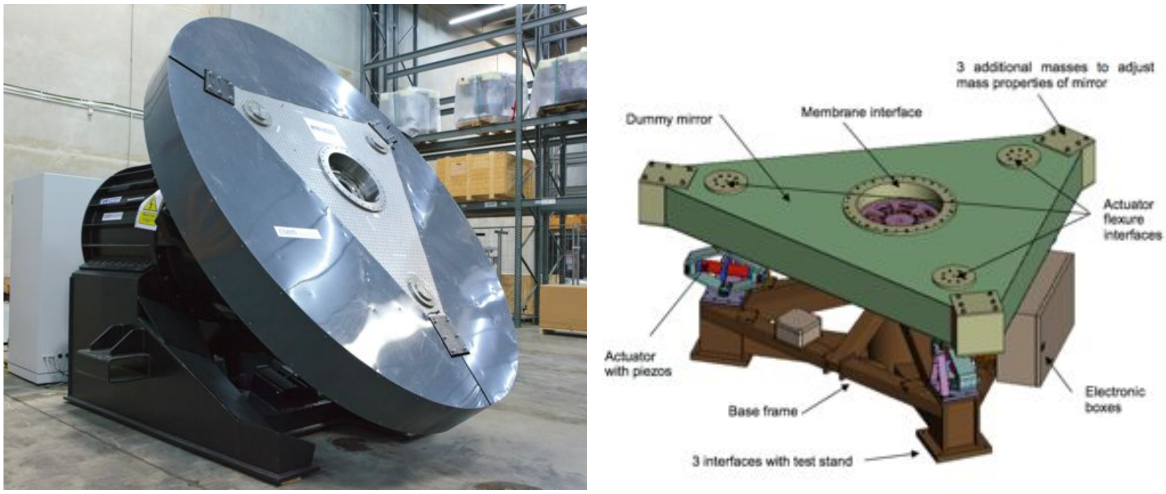

Figure 1. M5 scale-one prototype (left) and the overview (right)

position sensor. The total stroke of each actuator is 700-μm, a large portion of which is used for fine alignment and to compensate for gravity deformations and the remaining for the atmospheric and wind rejection.

The M5 unit scale-one prototype as designed by the contractor assumes a mirror with characteristics similar to a closed-back Ultra Low Expansion (ULE) mirror where the actuators are connected to the mirror without the need for an axial support system (whiffle tree). The mirror is restrained laterally using a central membrane. In the prototype a cut-out of an optical table with the same mass but lower eigen-frequencies has been used as dummy mirror. For tip-tilt control this does not affect the performance of the system which is dominated by the modes of the electro-mechanical part. If a open-back Zerodur mirror option is considered, a whiffle tree system with nine support points is necessary. Figure 2 compares the FEM representation of the M5 unit assuming a closed-back ULE with an open-back Zerodur mirror option.

Table 1. M5 mirror option main characteristics

Zerodur	495 kg ($90kg/m^2$)	open-back	first mode (free): 139Hz	9 point support
ULE	390 kg ($70kg/m^2$)	closed-back	first mode (free): 300Hz	3 point support

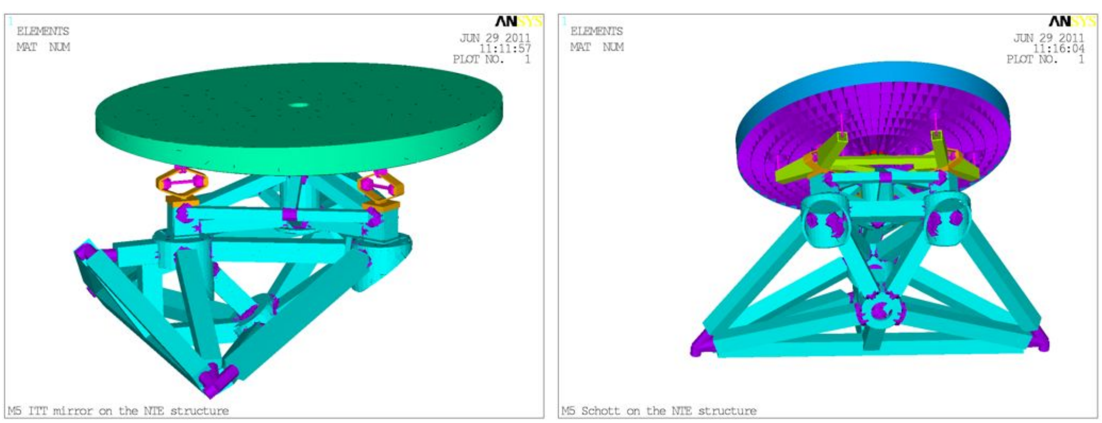

Figure 2. M5 FEM: closed-back ULE mirror (left), open-back Zerodur mirror with whiffle tree support (right)

To be able to meet the telescope requirements the unit from any tip/tilt command input to output shall exhibit sufficient bandwidth[6]. The required bandwidth can be guaranteed thanks to the local control loops of the electromechanical unit: i) an active damping loop, ii) a position control loop. A trade-off study and analysis was performed to answer the following main questions: Is the damping strategy efficient for all mirror options? Which modes limit the stability and robustness? Can the desired unit bandwidth of 10Hz be achieved robustly for all mirror options? What are the main active damping strategies and algorithms which can be considered? How do they compare? What are the main factors limiting the efficiency of the active damping of the unit? How does the mechanical interface of the unit to the telescope structure affect the control and performance of M5?

In this paper, a summary of the important results and conclusions of the analysis is presented. In Section 2 different damping strategies are introduced. The active damping strategies are tested on the dynamical model extracted from FE analysis and the results are compared in terms of efficiency and stability/robustness for two different unit mirror designs, i.e. closed-back ULE vs. open-back Zerodur. In Section 3 some measurement results on the scale-one prototype are presented, and the conclusions are given in Section 4.

2. ACTIVE DAMPING STRATEGIES AND MAIN RESULTS

2.1 FE Models for two mirror designs and comparison of the open-loop frequency responses

From a detailed FEM (capturing the mechanical modes up to 600Hz) of the M5 unit for the two mirror options, closed-back ULE (no whiffle tree) vs. open-back Zerodur (with three tripods for a nine-point support), the frequency responses of the actuator input command to a collocated sensor measuring the stroke of the actuator are derived. It is assumed that the unit is attached to an infinite stiff structure. The effect of the telescope structure was as well analyzed but the results are out of scope of this document. Figure 3 compares the open-loop responses for three actuators for ULE and Zerodur options respectively.

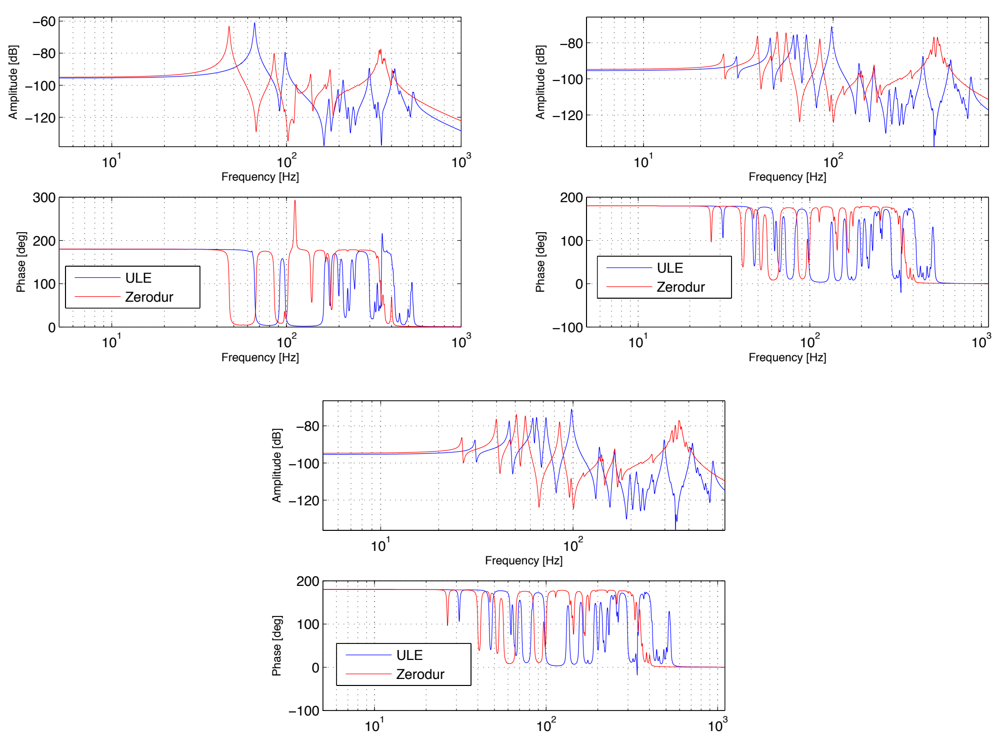

Figure 3. M5 ULE vs. Zerodur mirror design: Actuator open-loop frequency responses (input command force to local sensor), Act #1 (top left), Act #2 (top right), Act #3 (bottom)

Due to a non symmetric installation of actuators on the M5 unit one actuator response differs from the other two. The mechanical modes of the Zerodur mirror design option are lower in frequency. The first large amplitude mechanical mode seen by the sensor on Actuator #1 of ULE and Zerodur option designs are at 66Hz and 47Hz, respectively. Actuator #2 and #3 exhibit the same response with first visible mechanical mode (though small) at 31Hz and 26Hz for ULE and Zerodur designs, respectively. For ULE mirror the first largest amplitude mode is at 46Hz while for the Zerodur this mode is at 40Hz. For the ULE design a mode at 98Hz has an important amplitude while the similar mode for the other design option has a smaller amplitude. However, the Zerodur mirror option exhibits a large amplitude mode at 340Hz which is the local mode of the actuator ellipses and the whiffle tree tripods.

The requirement on M5 unit closed-loop bandwidth is 10Hz. For both mirror options the required robust stable closed-loop bandwidth cannot be achieved unless the first mechanical modes are damped or notched. The approach based on notch filters is disadvantageous since a good knowledge of the location of the problematic modes is required and in general is non-robust. In addition, while solving the problem of control it does not solve the problem of response to any perturbation excitation. In case of using an active damping strategy the location of the sensing system and control strategy plays an important role in damping of the harmful mechanical modes. In the next section different strategies and their outcome on the two mirror options are discussed. The models have the necessary inputs and outputs to perform the required trade-off analysis and control design: the inputs are the actuator forces and the outputs are considered to be the absolute or differential acceleration of actuators, the elongation of three actuators (position sensor), force at the interface of actuator and mirror (force sensors) together with 100 mechanical modes of the electromechanical unit.

2.2 Strategies and Results

The active damping strategies are classified based on the type of the sensors, their physical location and the type of the implemented algorithm.[7] In this work three main schemes on the basis of the sensing system for active damping are assumed: i) accelerometer, ii) force sensor, and iii) position sensor. In the case of accelerometer based active damping approach two possibilities were investigated: ia) accelerometers are located on the top of each actuator measuring the absolute signal, ib) two accelerometers are installed, on the top and bottom of each actuator, and the differential signal value is used for control.

One objective of the work is to evaluate the efficiency of the active damping schemes in face of problematic resonant modes of the unit. Therefore, to be able to compare mirror options, identical control parameters were implemented for different mirror options and for the same strategy. For each mirror design and damping strategy a Multi-Input Multi-Output (MIMO) robust stability criterion is verified [*]. In order to distinguish the effect of the cross-coupling and the control structure interaction on the robustness, the Single-Input Single-Output (SISO) sensitivity transfer function, e.g. for the tip response, is compared with that of the MIMO criterion. The control of the position loops are implemented in the piston/tip/tilt (PTT) space. Hence, a geometrical transformation projects the signals of actuator position sensors to the piston/tip and tilt of the M5 unit. The frequency responses from PTT input commands to the PTT generated from the local position sensors are used as a basis for design of three identical integral position controllers, $C_p = \frac{k_i}{s}$, for the piston/tip and tilt signals constructed from the position sensors. Assuming enough damping is introduced by the active damping the gain of $k_i = 56$ leads to a tip/tilt reference to output closed-loop bandwidth (-3dB) of 10Hz.

2.2.1 Acceleration Feedback

The strategy consists on either to integrate the acceleration signal a to obtain the velocity and then by a direct gain controller K_a introduce damping, i.e.

$$u = C_{damp} * a = -\frac{K_a}{s} * \frac{s}{s+\omega_b} * a = -\frac{K_a}{s+\omega_b} * a \tag{1}$$

[*]using the characteristic transfer functions CTFs, i.e. eigenvalues of the MIMO loop transfer matrix which take into account the dynamical cross-coupling and control and structure interactions,[8] and the infinity norm of the MIMO sensitivity transfer function

or by passing the acceleration signal through a second order filter and by generating a force proportional to the output of the filter, i.e.

$$u = C_{damp} * a = -\frac{K_a}{s^2 + 2\xi_f \omega_f s + \omega_f^2} * \frac{s}{s + \omega_b} * a \tag{2}$$

where damping factor ξ_f at a selected frequency ω_f are chosen by the designer.

In practice, acceleration signals at low frequencies are noisy and thus a high-pass filters are included in the controllers. The high-pass filter corner frequency is presented by ω_b.

Closed-back ULE mirror option: Figure 4 compares the tilt frequency response constructed from position sensors before and after implementing the active damping using the direct velocity Eq.(1) approach for both cases of accelerometer on the top of an actuator and the differential acceleration signal and for the closed-back ULE mirror option.

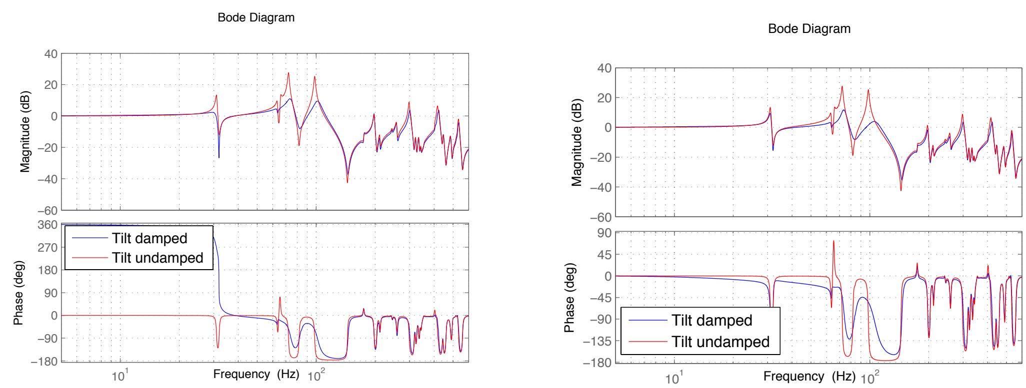

Figure 4. Closed-back ULE mirror: tilt frequency response before and after damping. Accelerometer on top of each actuator (left), Accelerometers on top and bottom of each actuator (right). Note: The large phase transition of 360deg is an artifact.

In the case of accelerometer on top of each actuator, the first 3 important modes are damped. Both the active damping and the position loops are MIMO robust stable (see Figure 5). Further investigation showed that mechanical modes at 100Hz could lead to stability issues for the damping loop and the non-damped mode at 31Hz could be problematic for the outer-loop (position) loop.

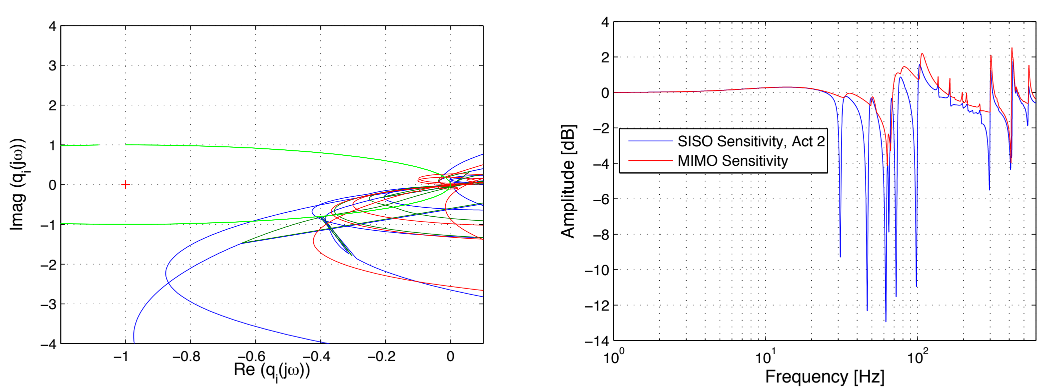

Figure 5. Closed-back ULE mirror active damping with accelerometer on top of each actuator: MIMO Nyquist curves (left) and Sensitivity transfer function $||S||_\infty$ (right) of the active damping loop.

When the accelerometer on top and bottom of each actuator are used (differential signal), one expects a perfect collocation and simply by increasing the damping loop gain better results can be obtained. Although this was verified, for the sake of comparison the results for the same control gains are presented here. In this case the important modes except the mode at 31Hz are damped. The active damping loop is robust stable. The position loop is stable, however due to the undamped mechanical mode at 31Hz and the cross-coupling effects the position loop is not robust, i.e. $||S||_\infty > 6$dB (see Figure 6).

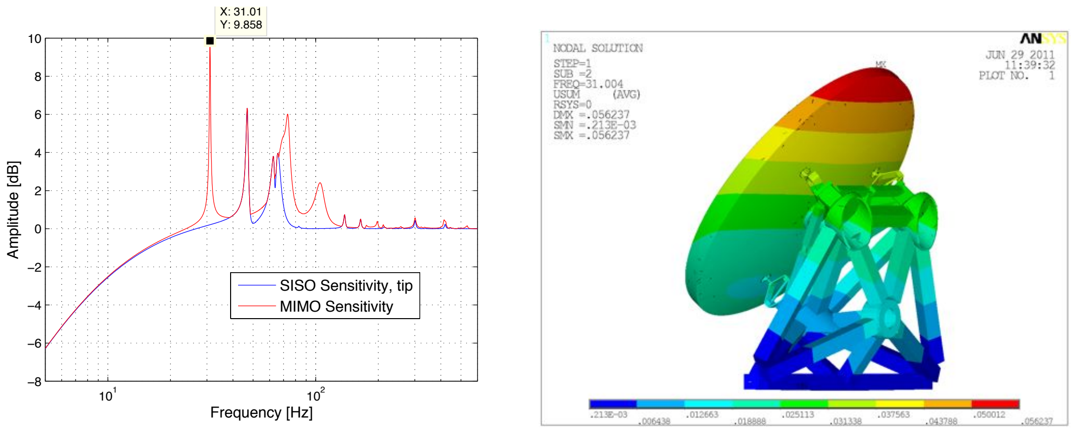

Figure 6. Closed-back ULE mirror active damping with accelerometer on top and bottom of each actuator: Sensitivity transfer function $||S||_\infty$ of the PTT position loop (left), Graphical representation of the mode at 31Hz (right)

The mode at 31Hz is mainly related to the tilt motion of the mirror together with the back structure. This is the main reason that the mode is not seen on the differential measurement and consequently cannot be damped by this strategy. The graphical representation of this mode is depicted in Figure 6. The results for the second order filter algorithm are similar and to avoid a repetition they are not presented here.

Open-back Zerodur mirror option: Figure 7 compares the piston frequency response constructed from position sensors before and after implementing the active damping using the direct velocity Eq.(1) approach for both cases of accelerometer on top of an actuator and the differential acceleration signal for the open-back Zerodur mirror option.

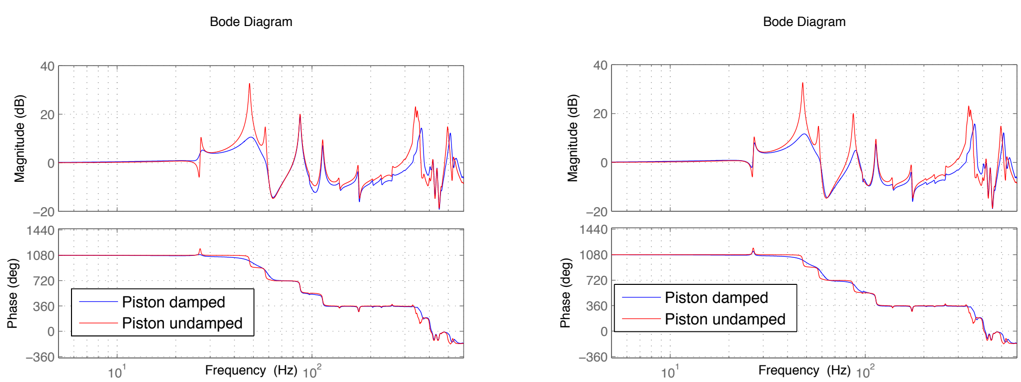

Figure 7. Open-back Zerodur mirror : piston frequency response before and after damping. Accelerometer on top of each actuator (left), Accelerometers on top and bottom of each actuator (right)

For this case and for accelerometer on the top of each actuator the first 3 important modes are damped. However, it can be seen from Figure 8 that the high frequency modes, e.g. mode at 366Hz, cause robustness issue for the damping loop. It was observed that in case of the accelerometer on the top of each actuator the mode at 86Hz (piston mode) is not damped and the system with the selected position loop gain becomes unstable. If the differential accelerometer signal is used instead, this mode is damped and hence no stability issue for the position loop is observed. However, the lowest mode at 26Hz is a global mirror support mode and is not seen by the differential accelerometer and is consequently not damped in this approach. As a results the position loop for the selected control gains and the desired bandwidth is not robust stable at this frequency. Similar results and observations were obtained in the case of the second order filter algorithm. To avoid the repetition they are not presented in this paper.

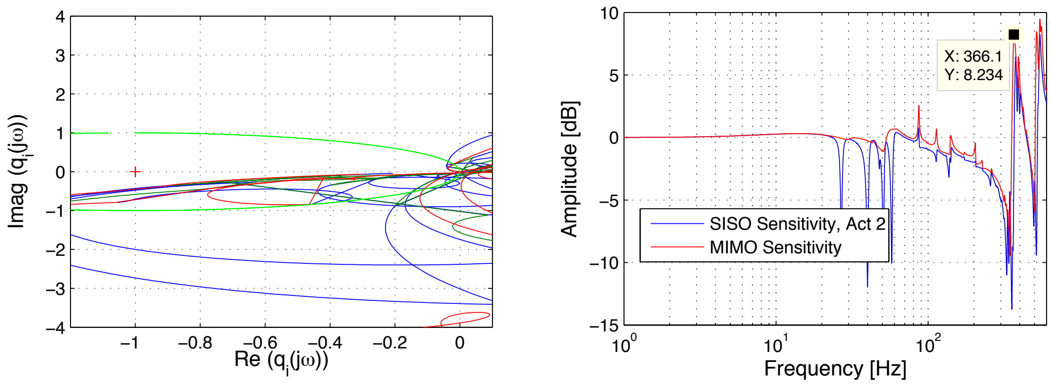

Figure 8. Open-back Zerodur mirror option: accelerometer on top of each actuator: MIMO Nyquist curves (left) and Sensitivity transfer function $||S||_\infty$ (right) of the active damping loop

2.2.2 Force feedback

The approach is more or less equivalent to the control strategies based on acceleration feedback. There are however some advantages with force feedback, i) force sensors have often better sensitivity than accelerometers, ii) the stability properties of the force feedback are often better than the acceleration feedback.[7] Let K_{act} be the axial stiffness of each actuator, then the force sensor y measures the force at the interface of the actuator and the mirror, i.e. $y = -K_{act}z + u_{act}$, where u_{act} is the active control force of an actuator. The controller is the integral of the measured force, i.e.

$$u = C_{damp} * y = -\frac{K_f}{s} * y \tag{3}$$

In practice often high-pass filters are added to the control to remove possible offsets and low frequency perturbations.

Closed-back ULE mirror option: Figure 9 compares the piston and tilt frequency responses constructed from position sensors before and after implementing the active damping using force feedback Eq.(3).

The active damping loop is stable and robust. However, due to non collocation the mode 410Hz limiting the efficiency of the damping loop and reduced the robustness (see Figures 9 and 10). The position loop is robust stable.

Open-back Zerodur mirror option: Figure 11 compares the piston and tilt frequency responses constructed from position sensors before and after implementing the active damping using force feedback Eq.(3). The damping is efficient for three of the important mechanical modes.

The active damping loop is stable and robust. However, due to non collocation the mode 355Hz limiting the efficiency of the damping loop and reduced the robustness . The position loop is consequently robust stable where the modes at 340Hz and 355Hz are the limiting modes. In comparison to the case of closed-back ULE mirror the high amplitude of the non damped high frequency parasitic modes are limiting the robustness of the position loop with the desired bandwidth of 10Hz.

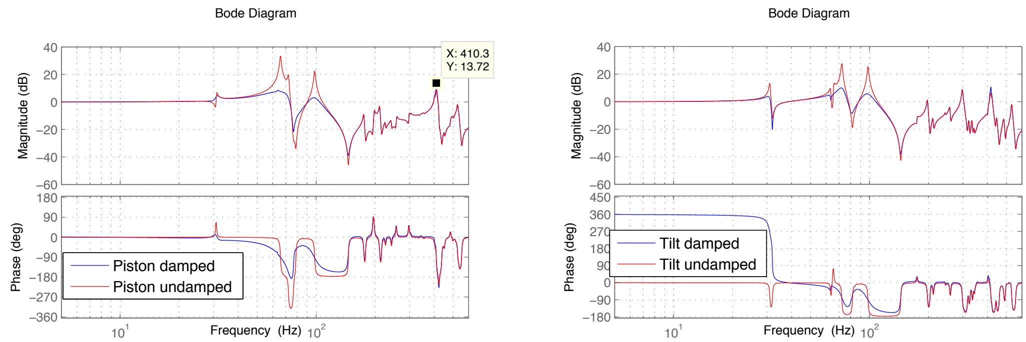

Figure 9. Closed-back ULE mirror with force feedback active damping: piston (left) and tilt (right) frequency responses before and after damping

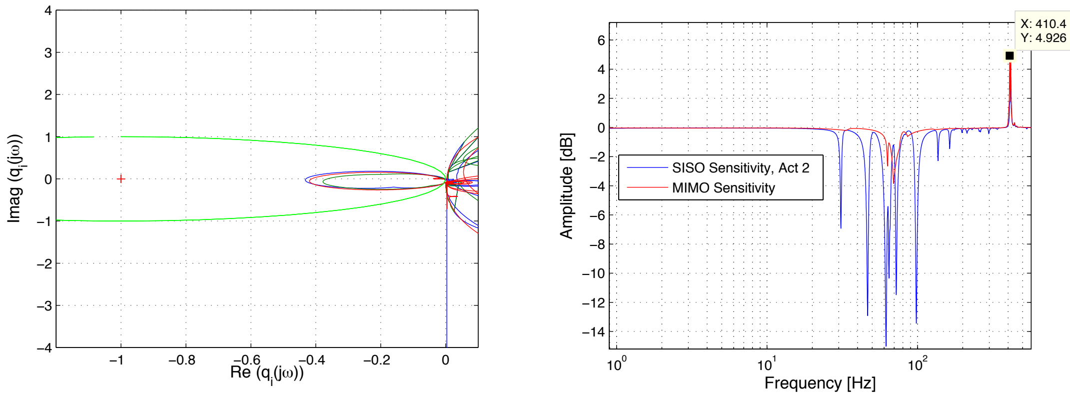

Figure 10. Closed-back ULE mirror with force feedback active damping: MIMO Nyquist curves (left) and Sensitivity transfer function $||S||_\infty$ (right) of the active damping loop.

2.2.3 Positive position feedback

The approach consist of filtering the position signal (from the position sensor) with a second order filter and feed it back to generate a force in a positive feedback constellation. This is not an intuitive approach while in general most of the control loops are negative feedback loops. The effect and damping capabilities are more or less like the acceleration based active damping strategies with an additional property that the control adds -40dB/decade roll-off at higher frequencies.[7] The filter has the frequency ω_f and the damping ξ_f as design parameters:

$$u = C_{damp} * z = +\frac{K_z}{s^2 + 2\xi_f \omega_f s + \omega_f^2} * z \tag{4}$$

where z is the position signal.

Closed-back ULE mirror option: Figure 12 compares the piston and tilt frequency responses constructed from position sensors before and after implementing the active damping using the positive position feedback (Eq. 4) for the closed-back ULE mirror option.

The damping is efficient for three of the important mechanical modes. The scheme changes the static gain of the inner-loop (see Figure 12). Therefore, to maintain the required position closed-loop bandwidth at 10Hz and in order to keep the position loop control gain identical for this case as for the other schemes, a scaling gain factor in addition should be applied .

The active damping loop is stable and robust. Note that due to the specific shape of the frequency response of this approach the range of suitable steady state gains is limited. The damping loop controller gain was adjusted

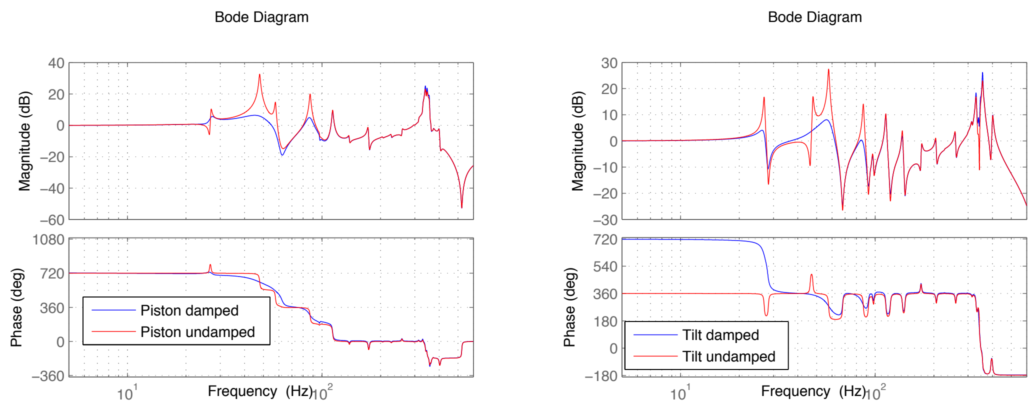

Figure 11. Open-back Zerodur mirror with force feedback active damping: piston (left) and tilt (right) frequency responses before and after damping

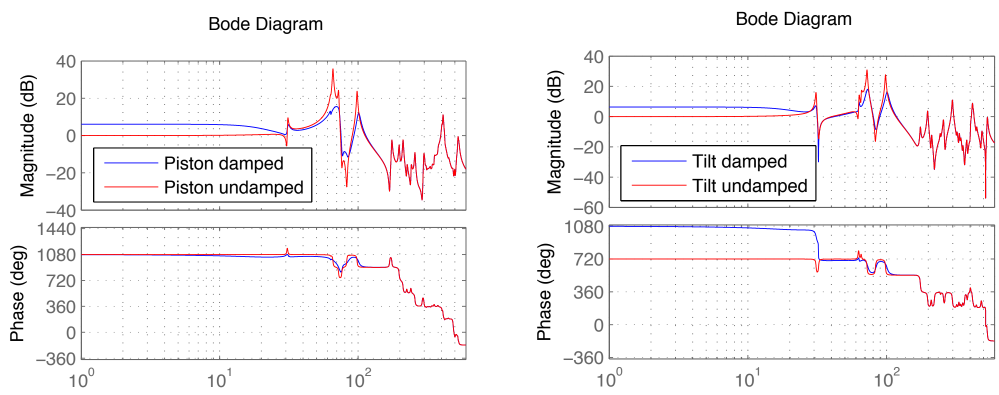

Figure 12. Closed-back ULE mirror with positive position feedback active damping: piston (left) and tilt (right) frequency responses before and after damping

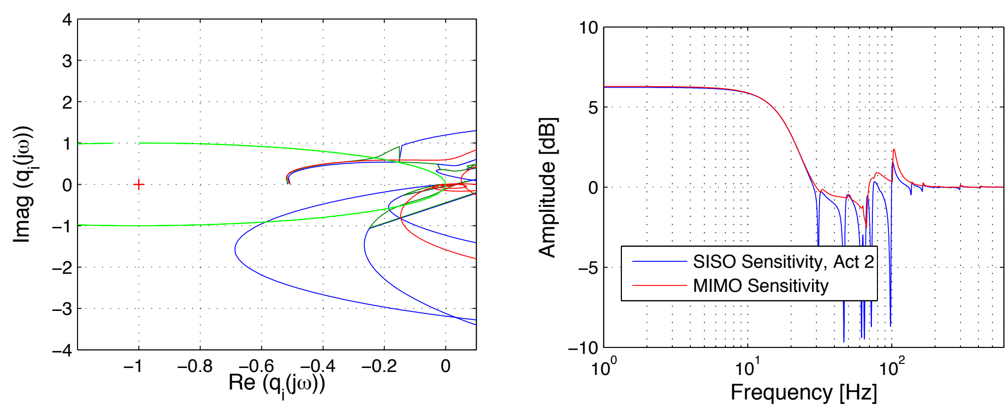

Figure 13. Closed-back ULE mirror with positive position feedback active damping: MIMO Nyquist curves (left) and Sensitivity transfer function $||S||_\infty$ (right) of the active damping loop.

such that the sensitivity gain remains under 6dB. The limiting robustness gains are mainly at low frequencies (see Figure 13). In general, at low frequency there are less uncertainties on the amplitude and phase of the system. Therefore, one could expect the damping loop gain can be increased without an important consequence on the stability of the design.

Open-back Zerodur mirror option: Figure 14 compares the piston and tilt frequency responses constructed from position sensors before and after implementing the active damping using the positive position feedback (Eq. 4) for the open-back Zerodur mirror option.

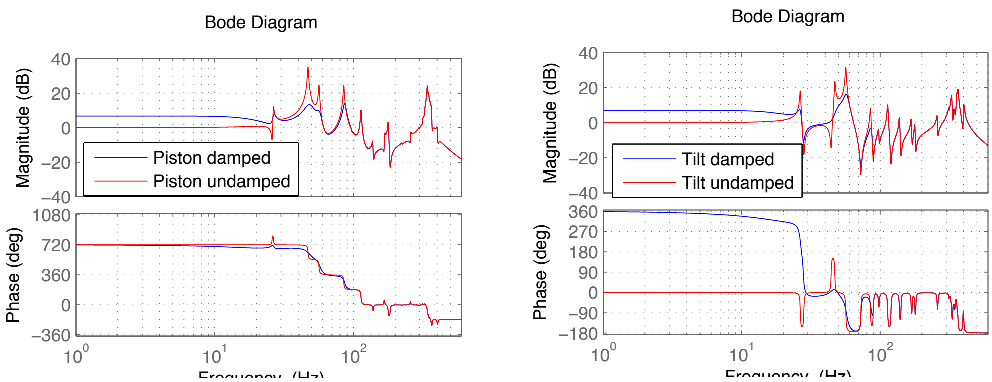

Figure 14. Open-back Zerodur mirror with with positive position feedback active damping: piston (left) and tilt (right) frequency responses before and after damping

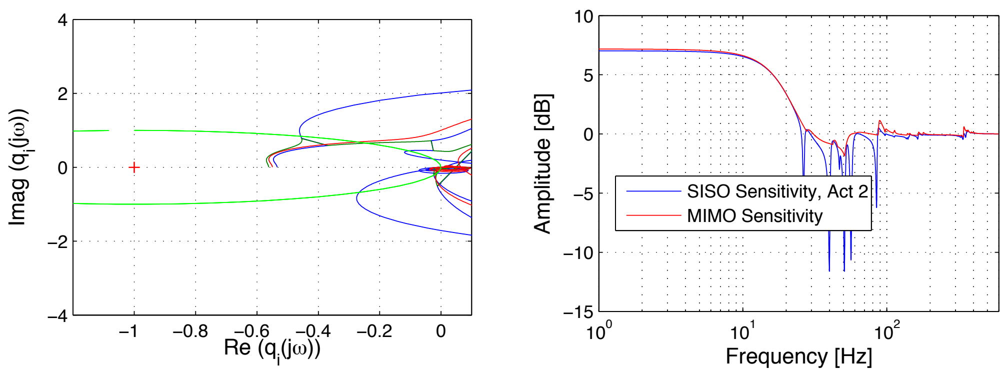

Figure 15. Open-back Zerodur mirror with positive position feedback active damping: MIMO Nyquist curves (left) and Sensitivity transfer function $||S||_\infty$ (right) of the active damping loop

The active damping loop is robust stable. The limiting robustness margins are mainly at low frequencies (see Figure 15).

3. MEASUREMENT RESULTS ON THE M5 PROTOTYPE UNIT

During a test period on M5 unit prototype the active damping strategy based on the velocity feedback using the accelerometer sensor was investigated. Different type of accelerometers and their location on the actuator were tested as well. After extensive measurements and comparisons it turned out that the most favorable accelerometer location to be the one with the accelerometer on top of the actuator on the position sensor support. Here, the results related to this case is presented. The test procedure consists of measuring the open loop frequency of the accelerometer and actuator position sensor before and after the implementation of the active damping loop:

Actuators under test were excited with band-limited random noise signals. Open-loop frequency responses with frequency range of 0-200Hz and 0-500Hz were measured. Additionally, the cross-power spectra (coherence) were measured in order to verify the measurement quality. The configurable high-pass filters in the accelerometer preamplifiers were set to 1Hz. From the measured frequency response of each actuator input command to the accelerometer a parametric model was identified which in turn was used as a basis of controller parameter tuning. The reference response was fit by an 18th order polynomial model using a least squares method. As shown in Figure 16 the model represents well all modes until 200Hz and it is minimum-phase.

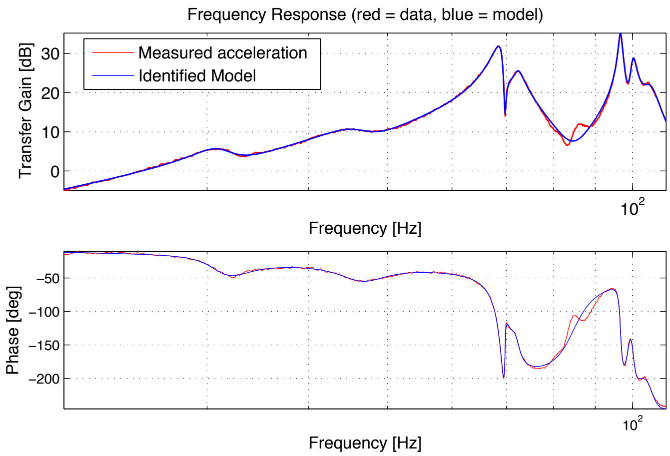

Figure 16. Measured accelerometer frequency response vs. identified model response

The tuning parameters were the gain and filter cut-off frequency K_a and ω_b as in Eq.(1). As a compromise between sufficient stability and robustness margins and sufficient damping (min. 10 dB for first resonant mode) a setting of $\omega_b = 2 * \pi * 10$Hz cut-off frequency and a gain of $K_a = 30$ was selected. To verify the stability and effect of higher order mechanical modes the system components (controller and controlled system) are represented by their frequency responses and the closed-loop frequency responses are calculated point-by-point over the complete frequency range of interest (here 0-500Hz).

The controller was implemented on the real time controller and the frequency response of the actuator input voltage to the position sensor was measured and compared with that of the open loop and expected response from the design. Figure 17 shows these measurement responses. In closed-loop response the 70Hz and 100Hz resonance modes were both damped to the extend predicted by analysis.

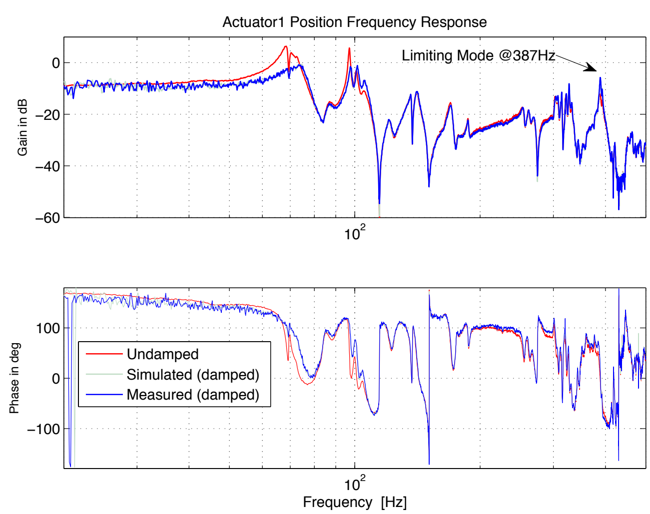

Figure 17. The effect of the active damping loop on the mechanical modes seen by actuator position sensor. Measured response before and after implementation of the active damping loop.

In order to explore the gain margin and the limitations due to model mismatch the feedback gain was increased until the system started to show tendency to oscillate. As shown in Figure 18, the increase in gain further improved the damping of the 70Hz and 100Hz modes. Further increase of gain led strong oscillations with a frequency of 387Hz.

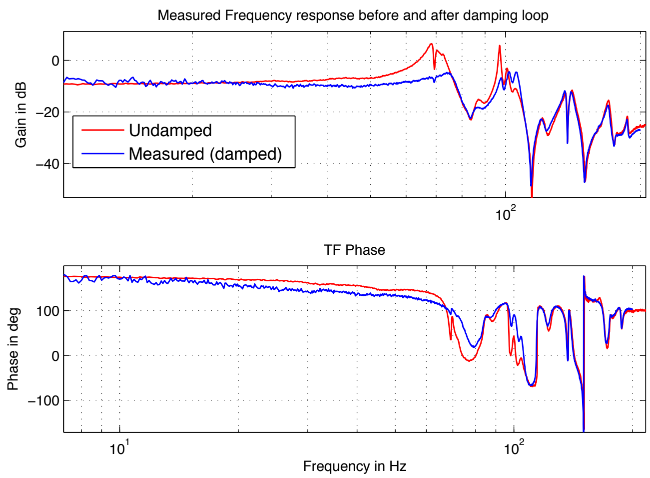

Figure 18. Strong damping on the main modes but at the limit of the stability

The nominal setting was also tested with the two other actuators. For both the active damping was stable and the first mode was damped like on actuator the first actuator.

4. CONCLUSION

From the analysis of different damping strategies and the two mirror options the following points can be concluded:

- All damping strategies discussed in the paper introduce damping to the main mechanical modes in the direction of sensing/control. Their efficiency, i.e. amount of the introduced damping, depends on the structural mechanical modes which are not damped (parasitic modes) or on the control/structure interaction combined with the effect of latency in the control system limiting the damping loop gain.
- Depending on the location of the sensor, e.g. absolute acceleration or differential, the parasitic modes affecting the efficiency of the damping loop differ.
- Due to the presence of higher number of parasitic modes with a higher amplitude (mostly high frequency) at the actuator and whiffle-tree interface, the damping loop for the open-back Zerodur mirror option is less robust and consequently less effective. Specifically, the approach with accelerometers are shown to be not efficient as in the case of closed-back ULE mirror.
- The difference between direct velocity feedback Eq.(1), and the second order filter of acceleration signal Eq.(2), are mainly algorithmic: the direct velocity feedback has one gain to tune while the second order filter scheme requires a prior knowledge on the frequency or frequency ranges where the damping should be efficient. The direct velocity feedback approach using accelerometer located of the top of the actuators was demonstrated successfully on the scale-one prototype. In the next measurement campaign the effect of the MIMO implementation (simultaneous operation of three damping loops) will be tested.
- The analysis showed that integral force feedback Eq.(3) is promising for both mirror options. The approach requires a force sensor located properly at actuator/mirror (whiffle-tree) interface. If the sensor is well collocated with the actuator the damping loop is well efficient. One advantage could be that the sensitivity

of the available commercial force sensors are often higher than the accelerometers. This approach is not foreseen to be tested on this prototype because it requires a major design modification to include the force sensors. It will be tested in an alternative test setup.

- The analysis showed that the positive feedback strategy Eq.(4) is promising for both mirror options. The loss of robustness at low frequencies is a drawback. However, in general the uncertainties at low frequencies are lower so lower stability margins can be tolerated. Since no addition sensor or modification to the actual system is required, it will be tested on the scale-one prototype.

REFERENCES

1. J. Spyromilio, "E-ELT telescope: the status at the end of detailed design," in *Ground-based and Airborne Telescopes III*, L. M. Stepp and R. Gilmozzi, eds., *Proc. SPIE* **7733**, 2010.
2. A. M. McPherson, E. T. Brunetto, P. Dierickx, M. M. Casali, and M. Kissler-Patig, "E-ELT update of project and effect of change to 39m design," in *Ground-based and Airborne Telescopes IV*, L. M. Stepp, R. Gilmozzi, and H. J. Hall, eds., *Proc. SPIE* **8444**, 2012.
3. M. Cayrel, "E-ELT optomechanics: overview," in *Ground-based and Airborne Telescopes IV*, L. M. Stepp, R. Gilmozzi, and H. J. Hall, eds., *Proc. SPIE* **8444**, 2012.
4. J. M. Casalta, J. Barriga, J. Arino, J. Mercader, M. S. Andrés, J. Serra, I. Kjelberg, N. Hubin, L. Jochum, E. Vernet, M. Dimmler, and M. Müller, "E-ELT M5 field stabilisation unit scale-1 demonstrator design and performances evaluation," in *Adaptive Optics Systems II*, B. L. Ellerbroek and et al, eds., *Proc. SPIE* **7736**, 2010.
5. P. Bouchilloux, F. Claeyssen, and R. L. Letty, "Amplified piezoelectric actuators: from aerospace to underwater applications," in *Smart Structures and Materials 2004*, E. H. Anderson, ed., *Proc. SPIE* **5388**, 2004.
6. B. Sedghi, M. Müller, H. Bonnet, and B. Bauvir, "Field stabilization (tip/tilt control) of E-ELT," in *Ground-based and Airborne Telescopes III*, L. M. Stepp and R. Gilmozzi, eds., *Proc. SPIE* **7733**, 2010.
7. A. Preumont, *Vibration Conrtrol of active structures, an introduction*, Kluwer academic publishers, 2nd Edition, 2002.
8. O. N. Gasparyan, *Linear and Nonlinear Multivariable Feedback Control*, John Wiley and Sons Ltd, 2008.